Journal of Oil Palm Research
DOI: https://doi.org/10.21894/jopr.2023.0024

NANOCELLULOSE SYNTHESIS BY ONE POT METHOD WITH Fe CATALYST AND GELATINE CAPPING AGENT

LIDYA ELIZABETH[1]; SUDRAJAT HARRIS ABDULLOH[1]; ANIS NURRAHMAYANI; SERLINA MULYANI[1]; MARIA YUNI MEGARINI CAHYONO[2] and IRWAN HIDAYATULLOH[1]*

ABSTRACT

Nanocellulose has recently drawn attention because of its outstanding physical and mechanical properties. Even though nanocellulose is already a ubiquitous material in research, its synthesis and agglomeration still hinder the process of commercialisation. A shorter process will provide savings for larger scale production, and adding a capping agent can facilitate storage and handling on a commercial scale. In this study, the synthesis of nanocellulose was carried out using a one-pot method where the delignification and hydrolysis of cellulose were carried out in the same reactor. Delignification and bleaching used 30% (v/v) H_2O_2 at 90°C for 5 hr. Meanwhile, hydrolysis using 8% (w/w) H_2SO_4 and 3% (w/w) of $Fe(NO_3)_3.9H_2O$ 0.22 M as a catalyst, held for 1 hr at 75°C, resulted in the lowest lignin composition 49.7% (w/w). Several analyses were carried out for the nanocellulose. TEM analysis showed the nanocellulose size from 5 to 70 nm. FTIR analysis showed that the nanocellulose was alike cellulose commercial. XRD analysis showed the crystallinity of nanocellulose is still relatively low (35.7%). The addition of a capping agent to nanocellulose showed a reduction of agglomeration for the ratio of nanocellulose to gelatin 1.00:0.75.

Keywords: agglomeration, delignification, empty fruit bunch, hydrolysis, nanocellulose crystallinity.

Received: 26 October 2022**; Accepted:** 3 May 2023**; Published online:** 14 June 2023.

INTRODUCTION

The importance of valorisation of cellulose and other fractions is a biorefinery concept. Biorefinery strategy has been identified as a critical element for the breakthrough of the emerging bioeconomy by offering a wide range of products from biomass. The uses of biomass feedstocks to generate biofuels, bioproducts and bioenergy in a biorefinery concept will have a tremendous social and economic impact at the regional level by maximising local resources to promote industry development, generate added value and create employment (Manzanares, 2020). Cellulose, as part of biomass, is one of the most abundant natural polymers on earth. It has been widely used due to its sustainability and good mechanical properties. Nanocellulose has recently gained attention because it has a high tensile modulus (138 GPa), which is higher than that of the S-glass (86-90 GPa) and comparable to Kevlar (131 GPa), rendering them good reinforcement for natural and synthetic polymer matrices (Liu *et al.*, 2015). Besides, nanocellulose has abundant hydroxyl groups on the reactive surfaces, enabling the hybridisation with diverse, active materials to obtain composite electrodes for supercapacitors and demonstrating excellent electrolyte absorption capability (Xiao *et al.*, 2022). In addition, nanocellulose fibres are commonly used as a biodegradable filler which could improve tensile strength (Owi *et al.*, 2019). Nanocelluloses are highly crystalline, depending on the treatment, such as chemical or

[1] Department of Chemical Engineering,
Politeknik Negeri Bandung,
Gegerkalong Hilir,
40559, West Java, Indonesia

[2] Faculty of Psychology,
Maranatha Christian University,
Surya Sumantri,
40164, West Java, Indonesia

* *Corresponding author e-mail: irwan.hidayatulloh@polban.ac.id*

mechanical processing of natural cellulose used for their preparation (Zhong *et al.*, 2021). In addition, its crystallinity can vary from 40%-70% depending on the natural source and the treatment procedure (Trache *et al.*, 2020).

Nanocellulose can be synthesized from wood pulp, plant fibres, microbial, sea creatures, fruit skin, fruit husks and agricultural products. It can be used as nanocomposites, paper making, coating additives, food packing and cosmetics (Liu *et al.*, 2015). Besides, it is used for components in sensing materials such as optical, fluorescence, colorimetric and electrochemical sensors. Moreover, it is also used as a nanofiller and dispersant for immobilising various metals. In addition, nanocellulose is applicable for photoluminescent, conductive nanomaterials, carbon-based nanomaterials and fluorescent biomolecules in sensors (Mousavi *et al.*, 2022).

Acid hydrolysis using sulphuric acid is the oldest process. A typical approach starts with alkali and bleaching pre-treatments followed by acid hydrolysis. Various techniques have been reported to obtain nanocellulose: improved chemical acid hydrolysis, mechanical treatment, oxidation methods, enzymatic hydrolysis, ionic liquid treatments, deep eutectic solvents, subcritical water hydrolysis and combined processes (Trache *et al.*, 2020). Several methods of nanocellulose synthesis have been conducted, starting from pre-treatments such as soxhletation (Vivian Abiaziem *et al.*, 2019), delignification such as alkali and bleaching treatment, and acid hydrolysis (Milanez *et al.*, 2019; Onkarappa *et al.*, 2020; Vivian Abiaziem *et al.*, 2019).

Even though nanocellulose is a ubiquitous material in research, its commercial application is still in process. Cellulose purification (removal of lignin and hemicellulose) is responsible for more than 95% of the total environmental impact of the process. Its effect is equivalent to 400 kg CO_2 per 1 kg of nanocellulose if the subproducts (lignin and hemicellulose) are considered raw materials for other applications that are very non-neglectable carbon footprints (Horta-velázquez and Morales-narváez, 2022). Various biomass-pre-treatment has been carried out. It consists of biological, physical, chemical and physicochemical treatment. Biological treatments such as microorganisms that release hemicellulose and/or lignin-degrading enzymes will lead to increasing cellulose accessibility in biomass materials**.** The physical pre-treatments included milling and ultrasound, while the chemical treatments included acid pre-treatment, alkaline pre-treatment, organosolv pre-treatment and ionic liquids (ILs) pre-treatment. In addition, physicochemical methods for biomass pre-treatment include Ammonia Fiber Extraction (AFEX), hydrothermal, steam explosion, liquid hot water, supercritical fluids (SCF) and ionic liquids (ILs). An excellent pre-treatment method is one that should minimize energy (Silveira *et al.*, 2015). For example, the high concentration of sulphuric acid to hydrolyse cellulose for the preparation of nanocellulose is difficult to remove and negatively affects the quality of nanocellulose (Zhao *et al.*, 2020). Therefore, a shorter process and mild conditions will provide savings on a larger scale.

Thus, this study aims to synthesize nanocellulose by the one-pot method. The method allows the manufacture of nanocellulose using several purification steps of chemical processes such as alkalization, bleaching, and several purifications carried out directly in the same pot. This method provides a more straightforward approach and is more efficient in terms of time-consuming for the synthesis of nanocellulose. Several studies have been conducted to produce nanocellulose by one-pot method from different raw materials using chromium (III) nitrate as a catalyst in an acidic medium under mild process conditions of the hydrolysis. Chen and Lee (2018) reported that the yield of extracted nanocellulose from solid waste (panax ginseng, spent tea residue, waste cotton cloth and old corrugated cardboard) ranged from 24.6% to 69.3% with a crystallinity index range from 62.2%-83.6% and average particle diameter of 15.6-46.2 nm. Nanocellulose from fruit residue (pear peel) as reported by Chen *et al.* (2019) had high crystallinity index of 85.7%, with a yield of around 23.7% and an average diameter of 20.5 ± 6.3 nm.

Meanwhile, nanocellulose from *Elaeis guineensis* empty fruit bunch (Chen *et al.*, 2017) reported was reported to have a yield approaching 42%, with a particle diameter of 51.6 ± 15.4 nm and a crystallinity index of 85.7%. Agglomeration was still observed in the morphology. It is well known that the source of nanocellulose will be affected by its properties (degree of crystallinity, crystal structure, morphology and particle size). Therefore, the one-pot method is promising for producing nanocellulose with excellent properties.

In this work, the synthesis of nanocellulose from OPEFB was carried out by the one-pot method, where the delignification using hydrogen peroxide and hydrolysis using a mild concentration of H_2SO_4 solution and iron metal as catalyst were carried out in the same reactor (Chen *et al.*, 2017). The use of Cr metal-based catalysts is replaced with Fe metal, which is abundantly available in nature and is cheaper. In addition, the use of Fe metal ion and the presence of H_2O_2 cause the Fenton reaction. Fenton reactions have shown excellent performance, such as mild-treatment, environmentally friendly and more effective in degrading lignocellulose. It could oxidize and attack the recalcitrance structure of lignocellulose (Wu *et al.*, 2019). The addition of a capping agent was utilised to reduce the agglomeration of cellulose. In this work, the synthesis of nanocellulose from

OPEFB was carried out by the one-pot method, where the delignification using hydrogen peroxide and hydrolysis using a mild concentration of H_2SO_4 solution and iron metal as catalyst were carried out in the same reactor (Chen *et al*., 2017).

MATERIALS AND METHODS

Materials

Oil palm empty fruit bunch (OPEFB) was bought from Polytech Corp. H_2SO_4 95%-97% the analytical grade was purchased from Merck and $Fe(NO_3)_3.9H_2O$ analytical grade was purchased from Sigma Aldrich. H_2O_2 30% (v/v) technical grade and gelatine biological reagents were bought from a local chemical mart.

Methods

Synthesis of nanocellulose by one-pot method. Before delignification and bleaching, OPEFB was rinsed and soaked in distilled water for 30 min to remove impurities. Then, it is dried at 60°C for 6.5 hr. Furthermore, OPEFB was ground until the size 230-325 mesh (45-65 μm). The flow of the pre-treatment of OPEFB is shown in *Figure 1*.

Delignification and bleaching were carried out by adding 100 mL of 30% (v/v) H_2O_2 into 5 g of OPEFB in a three necks round-bottomed flask. Reaction occurred at 90°C for 5 hr (You *et al.* 2016). After that, hydrolysis was carried out by adding 8% (w/w) H_2SO_4 and $Fe(NO_3)_3.9H_2O$ 0.22 M in the same reactor as delignification and bleaching (one-pot method). Reaction occurred for 1 hr at various temperatures, as seen in *Table 1*. Finally, the nanocellulose sample was neutralised and filtered. Then, the lignin content of pre-treated nanocellulose was analysed. Nanocellulose treatment by One Pot Method from OPEFB is shown in *Figure 2*.

Addition of capping agent on nanocellulose. A nanocellulose solution of 1% (w/w) was prepared by mixing 1 g solid nanocellulose in 100 mL distilled water. A gelatine solution of 1% (w/w) was prepared by mixing 1 g of gelatine powder in 100 mL distilled water. Nanocellulose and gelatine solution were stirred in a beaker glass for 1 hr with continuous mechanical stirring (400 rpm) at 30°C. After that, the sample was subjected to sedimentation test. The best results from the sedimentation test were indicated by the longest time that nanocellulose precipitated. Then, this was followed by TEM analysis. The process of adding gelatin to nanocellulose is presented in *Figure 3*.

Response Surface Methodology. In this study, the synthesis of nanocellulose was evaluated based on two independent variables: catalyst composition (% w/w) and temperature (°C), to determine optimal conditions for maximum nanocellulose yield and lowest lignin composition. In the process of optimisation and identifying the best potential product, a Central Composite Design (CCD), which is an experimental design model by RSM was used to investigate the optimum process variables for obtaining a higher yield of nanocellulose and lower lignin composition. It is more accurate instead the other model such as Box-Behnken Design model and it does not required to do a three-level factorial experiment to create a second-order quadratic model (Bhattacharya, 2021). 100 mL of 30% (v/v) H_2O_2 was added into 5 g OPEFB as delignification process. After 5 hr, 8% (w/w) H_2SO_4 and $Fe(NO_3)_3.9H_2O$ were added to the reactor. The $Fe(NO_3)_3.9H_2O$ catalyst composition varied from 0.172 % (w/w) to 5.828% (w/w), and temperature ranged from 54°C to 96°C. All experiments (13) were analysed to obtain the relationship between the response variables (yield and lignin composition).

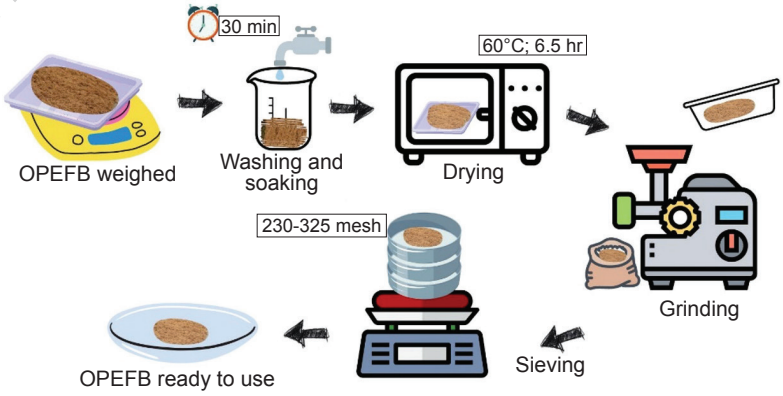

Figure 1. Pre-treatment of OPEFB.

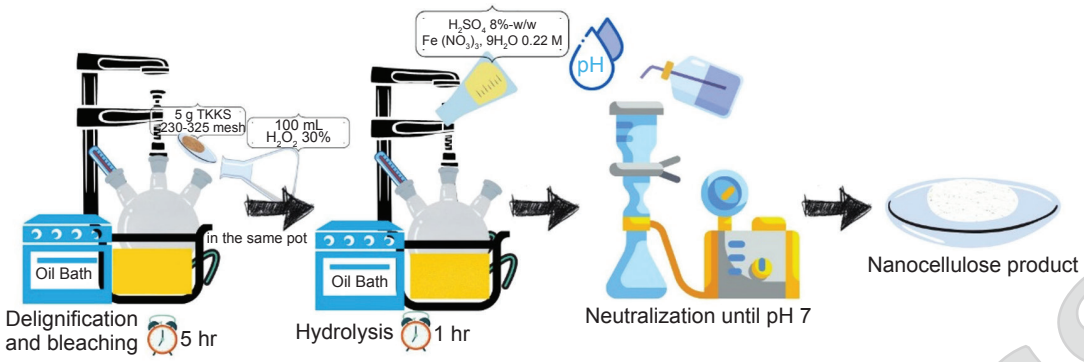

Figure 2 Nanocellulose Treatment by One Pot Method from OPEFB.

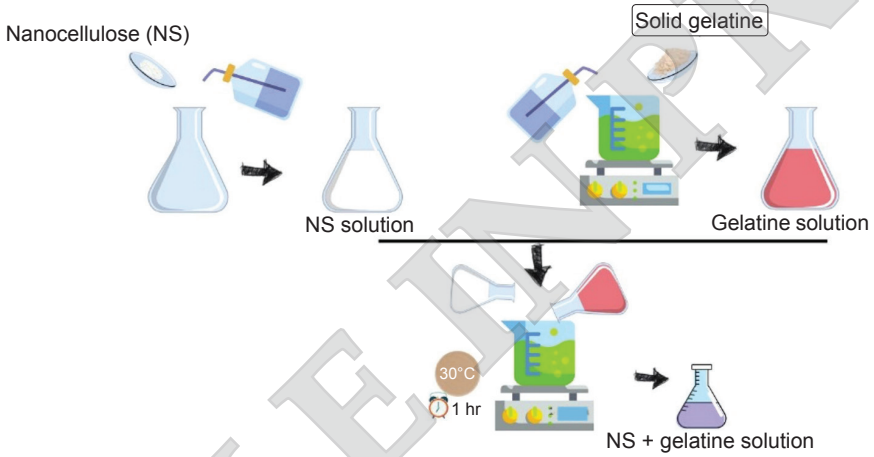

Figure 3. The process of adding gelatine to nanocellulose.

Characterisation of Nanocellulose.

Lignin composition by NREL method. 0.3 g of sample was mixed with 3 mL of H_2SO_4 72% (w/w) in an Erlenmeyer flask. It was hydrolysed in an incubator shaker at 30°C for 60 min. After incubation, 84 mL of distilled water was added to the solution for sterilisation in an autoclave for 15 min at 121°C. The sample was filtered to separate liquid and solid phases. The solid phase was dried in the oven at 105°C for 5 hr and measured as residue weight. After that, it was furnaced at 575°C for 4 hr and measured as ash weight. Spectrophotometer UV-Vis was used to analyse the filtrate phase at wavelength 205 nm to obtain lignin absorbance. Lignin composition calculation is presented in Equation (1) for acid-soluble lignin and Equation (2) for acid-insoluble lignin. Total lignin composition is the total composition of acid-soluble lignin and acid-insoluble lignin.

$$\text{acid-soluble lignin (\%-w)} = \frac{\text{absorbance x fitrate volume x dilution factor}}{\text{205 x sample dry weight x cuvette width}} \quad (1)$$

$$\text{acid-insoluble lignin (\%-w)} = \frac{(weight_{residue+dish} + - weight_{dish}) - \text{weight}_{ash+dish} - \text{weight}_{dish}}{\text{dry weight}_{sample}} \quad (2)$$

Sedimentation test. The sedimentation test shows the stability of the redispersed nanocellulose suspensions for determination of agglomeration. Suspensions of different nanocellulose samples were transferred to bottles and remained undisturbed every 4 hr for 24 hr (Velásquez-Cock *et al.*, 2018).

Fourier transform infrared spectroscopy (FTIR) analysis. Functional groups of nanocellulose were determined by FTIR (Shimadzu, types of Prestige 21) within the range of 500-4000 cm^{-1}. It was blended with KBr powder and shaped into a pellet.

Transmission Electron Microscope (TEM) analysis. TEM is the most helpful technique for nanocellulose size and morphology characterisation because it is readily available, cost-effective, and allows fast analysis of nanocellulose in solution as well as embedded in soft matter (Laura *et al.,* 2020). Nanocellulose was analysed by TEM (HT7700) at various voltages until a maximum of 120 kV. It was measured in solution form with distilled water as a solvent.

X-Ray Diffraction (XRD) analysis. X-Ray Diffraction (XRD) Bruker D8 Advance was used to analyse the crystallinity of nanocellulose. Analysis was determined at 40 kV and 40 mA. Samples were scanned in the range of 2θ from 10.00° to 90.00° with a scanning rate of 0.02°/min at room temperature.

Particle Size Analyser (PSA). PSA analysis was carried out using the Horiba SZ-100 (Z-Type), with a scattering angle of 90°, a dispersion medium viscosity of 0.897 mPa.s, and a distribution form polydisperse.

RESULTS AND DISCUSSION

Experimental Result

The correlation between yield and lignin composition of nanocellulose with process variables using RSM was evaluated. The experimental design matrix together with the result and predicted values of the experiment are presented in *Table 1*.

Effect of process parameters on yield of nanocellulose. In the acid hydrolysis process, the hydronium ion enters the amorphous regions of cellulose chains and promotes the hydrolytic cleavage of the glycosidic bonds. The benefit of using sulphuric acid as hydrolysing agent is that it initiates the cellulose surface esterification process and encourages the grafting of anionic sulphate ester groups. Furthermore, the presence of anion groups induces the formation of a negative electrostatic layer on the surface of the nanocrystals and helps their dispersion in water (Horta-velázquez and Morales-narváez, 2022).

Table 1 shows that the highest yield of nanocellulose is 40.12% (w/w), which is similar to the research conducted by Chen *et al.* (2017). It occurred when hydrolysis was conducted at 54°C and 3% (w/w) catalyst composition. For example, for a 3% (w/w) catalyst composition, an increase in temperature from 75°C [yield 15.00% (w/w)] to 96ºC [yield 12.95% (w/w)] decreases the yield of nanocellulose. The average decrease in yield of nanocellulose due to increasing temperature is 25%-27% (w/w). These results show that temperature of hydrolysis together with dilute acid impacts nanocellulose production. At the temperature between 75°C-96°C, hydrolysis treatment using Fe catalyst and dilute H_2SO_4 could degrade and disrupt lignocellulose material. Therefore, hydrolysis should be carried out at temperatures below 75°C. Further research must be conducted to examine which compounds are degraded at this hydrolysis temperature.

TABLE 1. RESULTS FOR CENTRAL COMPOSITE DESIGN MATRIX AND EXPERIMENT

Run	Actual values		Nanocellulose yield (% w/w)	Lignin composition (% w/w)
	Catalyst composition (% w/w)	Temperature (°C)		
	Before treatment			45.58
1	3.000	75	19.82	41.29
2	1.000	90	11.19	23.56
3	3.000	75	15.3	39.62
4	3.000	75	15.86	14.51
5	0.172	75	28.42	8.73
6	5.000	60	34.02	7.24
7	3.000	75	15.20	9.70
8	3.000	96	12.95	23.54
9	3.000	75	12.69	4.97
10	1.000	60	26.01	12.31
11	5.828	75	18.58	31.25
12	5.000	90	13.8	42.82
13	3.000	54	40.12	17.09

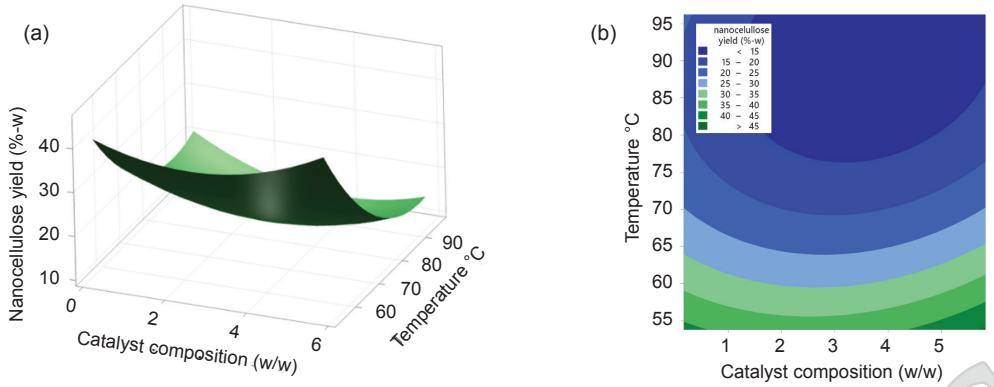

Figure 4. (a) Surface Plot of nanocelullose yield and (b) Contour Plot of nanocelullose.

Table 1 also shows that the increasing catalyst composition could reduce the yield of nanocellulose. For the same temperature (75°C), increasing the catalyst composition from 0.172% to 3.000%, will lower the yield of nanocellulose to almost half of the initial yield. Fe catalyst via the Fenton reaction plays a role in catalysing the breaking of lignocellulosic bonds. In the hydrolysis process, iron metal rapidly initiates and catalyses the decomposition of hydrogen peroxide, resulting in the generation of OH radicals. The reaction involves the oxidation of iron (II) to iron (III) by hydrogen peroxide and then the reduction of iron (III) to iron (II) (Wu *et al.*, 2019). It happened simultaneously, where the greater the amount of iron metal was included, more of the radicals were formed. It could accelerate and enhance lignocellulosic structure degradation. It is possible that not only lignin and hemicellulose bonds are broken but also cellulose. In the literature, the yield was less than the average cellulose composition.

The combination effect of catalyst composition and hydrolysis temperature can be seen in *Figure 4* and *Table 2*. In *Figure 4b* the interaction of the hydrolysis temperature and catalyst composition within the experimental domains examined, the effect was statistically insignificant. This can be seen from the *p*-value (0.553) of two-way interaction between catalyst composition and hydrolysis temperature on yield is higher than (0.05). When viewed from each parameter, the hydrolysis temperature has a significant effect (*p*-value 0.001), while the composition of the catalyst has a statistically insignificant effect (*p*-value 0.796). This can be seen in the fixed catalyst composition. The yield changes along with changes in hydrolysis temperature. Meanwhile, at a fixed hydrolysis temperature, the yield does not change with changes in the composition of the fixed catalyst. It can be concluded that the hydrolysis temperature is statistically significant to the yield of nanocellulose. However, the effect of the catalyst composition is statistically insignificant, as shown herein.

TABLE 2. ANALYSIS OF VARIANCE FROM NANOCELULOSE YIELD

Source	*p*-value
Model	0.006
Linear	0.002
Catalyst composition (w/w)	0.796
Temperature (°C)	0.001
Square	0.051
Catalyst composition (w/w)*catalyst composition (w/w)	0.119
Temperature(oC)*temperature (°C)	0.031
2-Way Interaction	0.553
Catalyst composition (w/w)*temperature (°C)	0.553
Error	
Lack-of-Fit	0.071

Effect of process parameters on lignin content of nanocellulose. *Figure 5* shows that catalyst composition and temperature are statistically significant to the lignin composition. The more significant amount of catalyst composition and the lower the hydrolysis operating temperature, the lower the lignin content produced. The hydrolysis process is carried out in the same pot. The addition of $Fe(NO_3)_3.9H_2O$ catalyst and the difference in temperature during hydrolysis caused changes during the process. *Figure 5* shows that when hydrolysis (catalyst composition 4%-5% w/w) is carried out at low temperatures (54°C-60°C), resulting in a low value of lignin composition; however, at high temperatures (75°C-96°C), the lignin composition produced is high. This is possible because the Fenton reaction during hydrolysis at high temperatures can degrade various lignin derivative compounds. In addition, Trache *et al.* (2020) also said that dilute acid use could increase inhibitor compounds with an increase in temperature reaction.

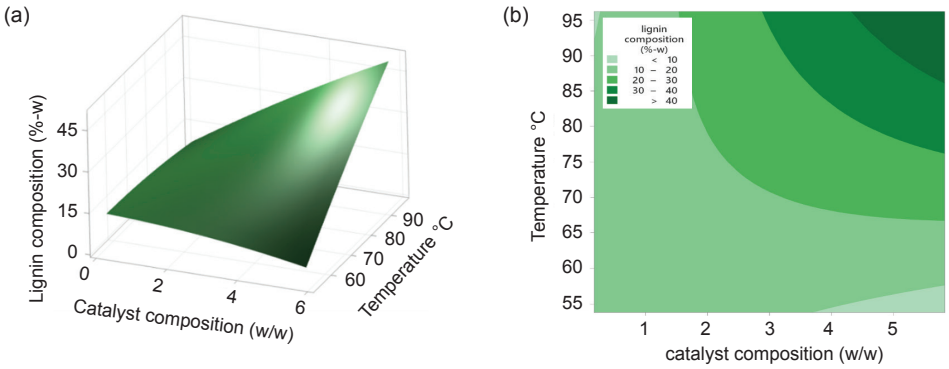

Figure 5. (a) Surface Plot of lignin composition and (b) Contour Plot of lignin composition.

TABLE 3. ANALYSIS OF VARIANCE FROM LIGNIN COMPOSITION

Source	*p*-value
Model	0.578
Linear	0.260
Catalyst composition (w/w)	0.288
Temperature (°C)	0.205
Square	0.989
Catalyst composition (w/w)*catalyst composition (w/w)	0.902
Temperature(°C)*temperature (°C)	0.926
2-Way interaction	0.418
Catalyst composition (w/w)*temperature (°C)	0.418
Error	
Lack-of-Fit	0.859

The combination effect of catalyst composition and hydrolysis temperature can be seen in *Figure 5* and *Table 3*. *Figure 5b* shows that the hydrolysis temperature and catalyst composition interaction have a statistically insignificant effect within the studied experimental domains. This can be seen from the *p*-value (0.418) of the two-way interaction between catalyst composition and hydrolysis temperature on the yield which is higher than (0.05). Each parameter has a statistically negligible effect. It can be seen from *p*-value of the hydrolysis temperature of 0.205 while the composition of the catalyst is 0.288. It can be concluded that the hydrolysis temperature and catalyst composition have a statistically insignificant impact on the lignin composition of nanocellulose. Regardless of the statistical analysis, valorisation of lignin from nanocellulose gave the lowest lignin composition at temperatures above 90°C and catalyst composition of 4%-5%.

Figure 6 shows the colour change due to the addition of $Fe(NO_3)_3.9H_2O$ catalyst. The solution remains light yellow when a small amount of $Fe(NO_3)_3.9H_2O$ catalyst is added. However, the solution turned green when more than 5% $Fe(NO_3)_3.9H_2O$ was added.

Characterisation of Nanocellulose

Sedimentation test. This analysis was conducted to determine the agglomeration of nanocellulose. Agglomeration can be seen from the fast and ease settling of nanocellulose.

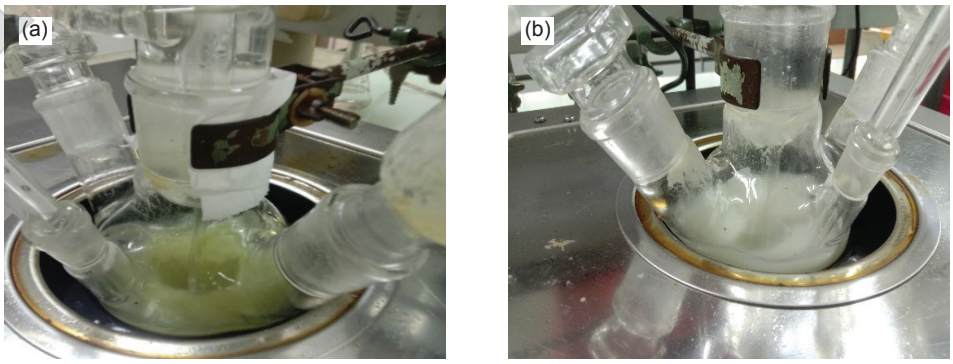

Figure 6. Hydrolysis with addition of catalyst $Fe(NO_3)_3.9H_2O$ (a) 0.0172% (w/w) and (b) 5.828% (w/w).

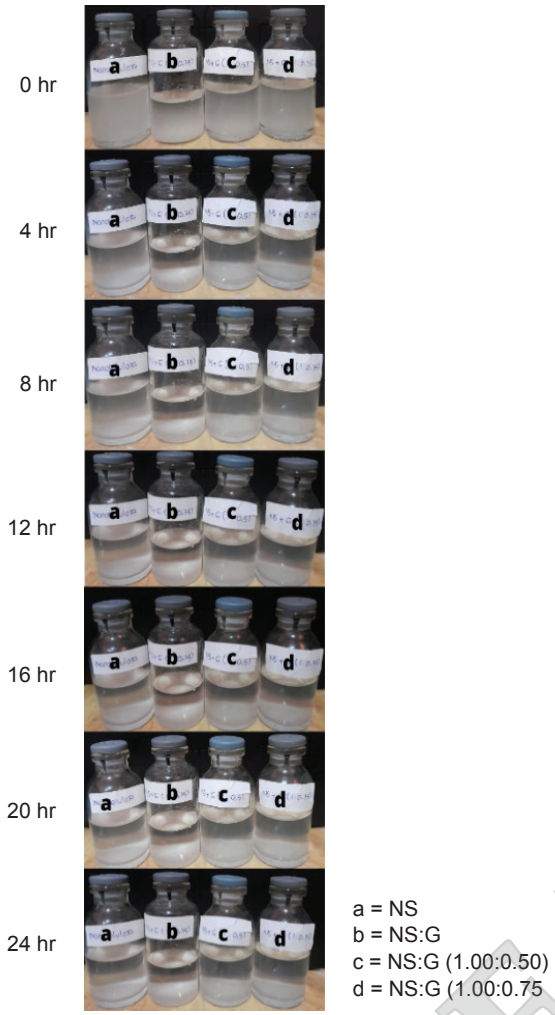

Figure 7. Sedimentation analysis of nanocellulose.

NS:G 1.00:0.75 (*Figure 7d*) showed better results compared to NS:G (*Figure 7a*), NS:G 1.00:0.25 (*Figure 7b*), and NS:G 1.00:0.50 (*Figure 7c*). The addition of gelatin causes the solution to be dispersed to prevent agglomeration of the nanocellulose. The drying process of nanocellulose at high temperatures causes the formation of hydrogen bonds. It causes agglomeration. However, when gelatin is added, the gelatin between the nanocellulose forms hydrogen bonds with each nanocellulose so that hydrogen bonds can be constrained when the water evaporates. It can prevent agglomeration. The more gelatin is added to the nanocellulose, the less possibility for it to agglomerate because the gelatin causes the solution to disperse easily.

FTIR analysis. The results of the FTIR analysis of nanocellulose (*Figure 8*) showed similarities to commercial cellulose. Peaks around 3400 cm^{-1} refer to the presence of O-H groups in the cellulose. Meanwhile, 2908 cm^{-1} refers to intermolecular hydrogen bonding in the -OH peak (Onkarappa *et al.*, 2020). It shows that the cellulose content is very high while the hemicellulose and lignin content has been much reduced.

TEM analysis. The sulphuric acid hydrolysis could cleave the amorphous region of microfibrils longitudinally, which causes a diameter reduction from micron to nanometers (Onkarappa *et al.*, 2020). *Figure 9* shows that the resulting nanocellulose has a 5-70 nm size range. The addition of gelatin can reduce agglomeration. It can be seen from the very small nanocellulose (5-15 nm). However, some agglomeration of nanocellulose can be observed in some places, while the rest are separated. Agglomeration still occurs, as indicated by the presence of a large nanocellulose (70 nm).

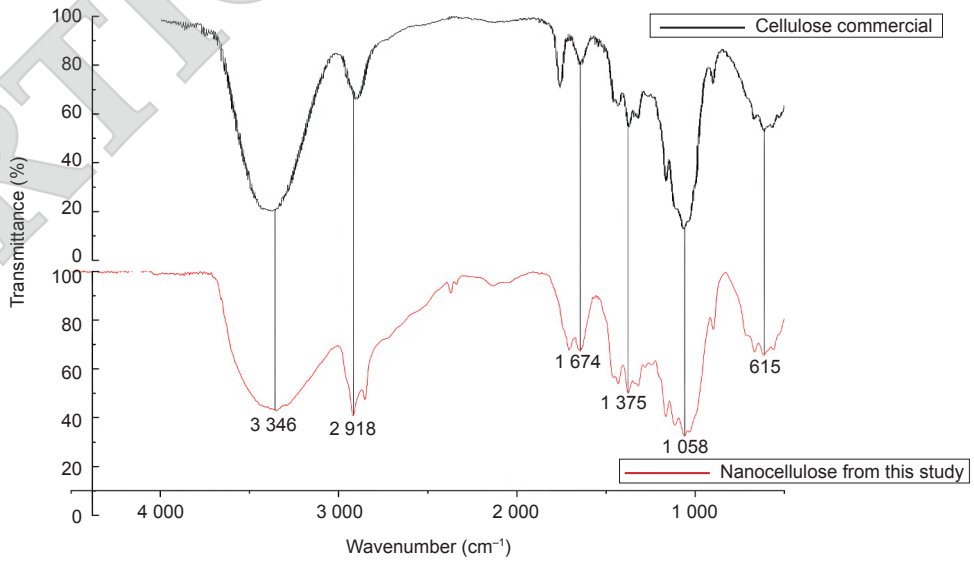

Figure 8. Cellulose commercial FTIR (Abderrahim et al.*, 2015) and nanocellulose FTIR from this study.*

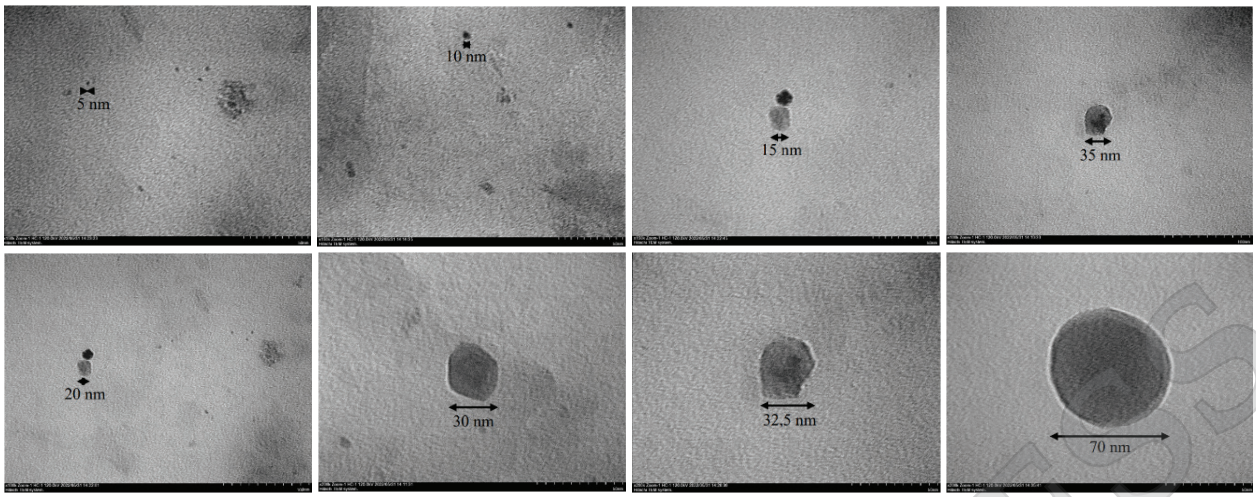

Figure 9. TEM analysis of nanocellulose.

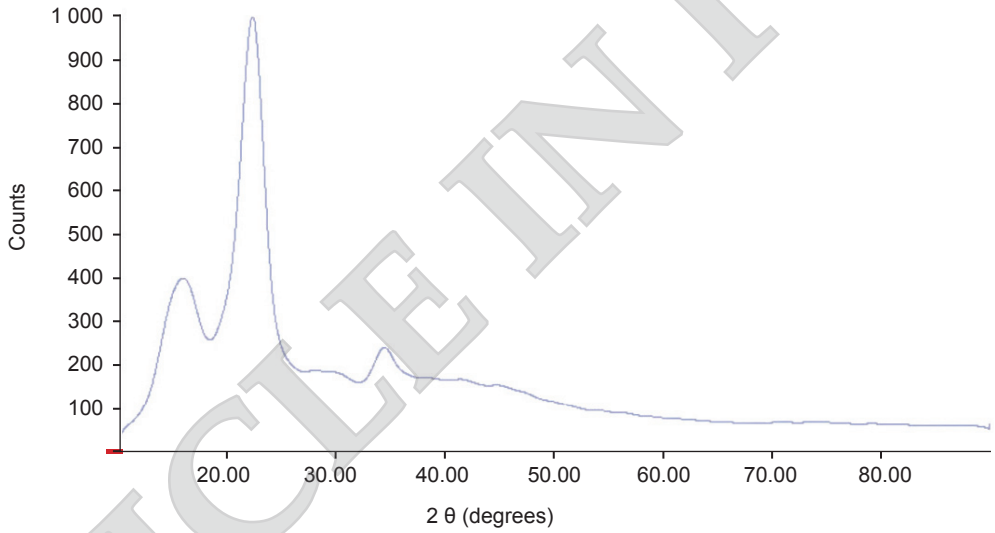

Figure 10. X-ray diffraction patterns of nanocellulose.

XRD analysis. A high crystallinity cellulosic material is essential due to thermal and mechanical resistance (Milanez *et al.*, 2019). XRD analysed nanocellulose to determine the crystallinity of nanocellulose. The result of the XRD analysis is presented in *Figure 10*. The area of crystalline regions is at 2 14.6º; 22.5º and 34.5º respectively meanwhile amorphous region area are at 2 21.5º (Chen *et al.*, 2017).

XRD analysis showed the degree of crystallinity was 35.7%, while the amorphous content was 64.3% (w/w). This value is smaller than the research of Wulandari *et al.* (2016), with a degree of crystallinity of 67.0%-76.0% produced by delignification using NaOH and hydrolysis using 50%-60% of H_2SO_4 solution. The crystallinity of nanocellulose is influenced by the concentration of acid. The higher the concentration of acid used during hydrolysis, the lower the degree of crystallinity (Wulandari *et al.*, 2016). Research conducted by Milanez *et al.* (2019) showed that cellulose's crystallinity was reduced with increase of acid concentration during hydrolysis. The concentration range was 50%-64% (v/v), resulting crystallinity index (CI) of nanocellulose was 75%-79%. Nanocellulose from the one-pot process produced a CI of 80.3% while using alkaline delignification and acid hydrolysis, resulting in CI of 75.4% (Chen *et al.*, 2017). The low crystallinity of nanocellulose in this study could

be due to the temperature, time, and the use of Fe metal as a strong oxidising catalyst, which probably contributed to the decrease of crystalline parts of cellulose chains.

PSA analysis. PSA analysis showed that the average size of nanocellulose particles was 706.9 nm with a size range of 247.0-315.0 nm and 2223.0-3621.0 nm. The particle size distribution is presented in *Figure 11*. The average particle size is out of the nano size range which could be due to the agglomeration of nanocellulose.

This agglomeration is thought to be caused by two factors. First, the final treatment, such as separating nanocellulose solids from the solution, neutralising, drying and storing, could stimulate agglomeration. Further research on the centrifugation method during neutralisation and separation is recommended for the final treatment. Second, agglomeration occurs because the crystallinity of nanocellulose is low. Meanwhile, mechanical resistance is related to crystallinity.

Particle size measurement. The measurement of nanocellulose particle size using TEM showed that some of the nanocellulose was small in the 5-70 nm range. This value is still lower than the particle size from Chen *et al.* (2017), which is 51.6 nm. However, the measurement of nanocellulose particle size by PSA showed that some of the resulting nanocellulose is also in a reasonably extensive size range, namely 247-3621 nm.

CONCLUSION

Nanocellulose was successfully obtained via a one-pot process consisting of delignification, bleaching and hydrolysis. The reaction is catalysed by iron metal, which is widely available in nature and uses mild acid concentration for hydrolysis. Surprisingly, the nanocellulose obtained was very good, as shown by several nanocellulose sizes of 5-70 nm. The work proved that Fenton reactions showed excellent performance and were effective in degrading lignocellulose in an acidic solution. However, agglomeration was still found after adding a gelatine capping agent. It is indicated by the average size of 247-315 nm and a large size of up to 3 μm. The nanocellulose produced was quite good, with the highest nanocellulose yield content of 40.12% (w/w) and the lowest lignin of 4.97% (w/w). FTIR analysis showed that the amount of cellulose was quite large, indicated by the similarity in the functional groups of the nanocellulose obtained when comparing with FTIR of commercial nanocellulose. The crystallinity of nanocellulose is still relatively low at 35.70% (w/w). Therefore, further research is suggested to verify the operating conditions to maintain the crystallinity of nanocellulose. Adding a capping agent to nanocellulose has been shown to reduce agglomeration of nanocellulose. The best results were obtained at the NS composition ratio: 1.00:0.75. Agglomeration still exists in the nanocellulose after the capping agent is added. Therefore, other methods to reduce agglomeration still need to be studied.

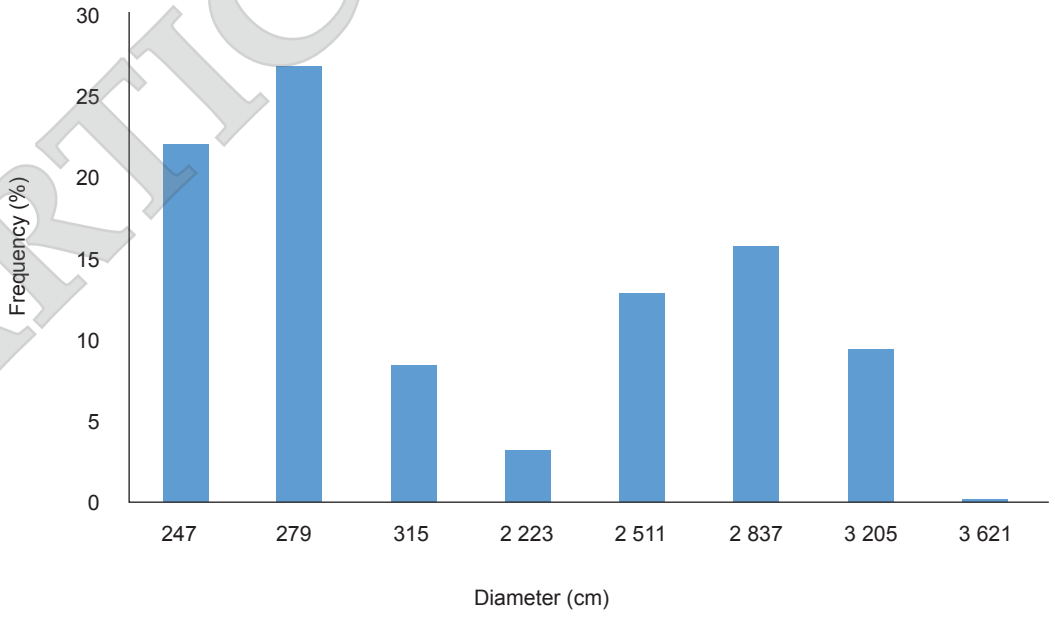

Figure 11. PSA analysis.

ACKNOWLEDGEMENT

The authors are grateful for the funding support of the Penelitian dan Pengabdian Masyarakat (P3M) Polban with contract number B/114.111/PL1.R7/PG.00.03/2022.

REFERENCES

Abderrahim, B; Abderrahman, E; Mohamed, A; Fatima, T; Abdesselam, T and Krim, O (2015). Kinetic thermal degradation of cellulose, polybutylene succinate and a green composite: Comparative study. *World J. Environ. Eng., 3(4)*: 95-110.

Bhattacharya, S (2021). Central composite design for response surface methodology and its application in pharmacy. *Response Surface Methodology in Engineering Science*. IntechOpen, United Kingdom. 1-19 pp.

Chen, Y W, Hasanulbasori, M A, Chiat, P F and Lee, H V (2019). *Pyrus pyrifolia* fruit peel as sustainable source for spherical and porous network based nanocellulose synthesis via one-pot hydrolysis system. *Int. J. Biol. Macromol.*, *123*: 1305-1319.

Chen, Y W and Lee, H V (2018). Revalorization of selected municipal solid wastes as new precursors of "green" nanocellulose via a novel one-pot isolation system: A source perspective. *Int. J. Biol. Macromol.*, *107* (PartA): 78-92.

Chen, Y W; Lee, H V and Abd Hamid, S B (2017). Facile production of nanostructured cellulose from *Elaeis guineensis* empty fruit bunch via one pot oxidative-hydrolysis isolation approach. *Carbohydr. Polym.*, *157*: 1511-1524.

Horta-velázquez, A and Morales-narváez, E (2022). Nanocellulose in wearable sensors. *Green Analytical Chemistry, 1(March)*: 100009.

Laura, C E; Alexandre, S and Liliane, C (2020). Specimen preparation optimization for size and morphology characterization of nanocellulose by TEM. *Cellulose, 27(9)*: 5435-5444.

Liu, D Y; Sui, G X; Bhattacharyya, D and Zealand, N (2015). Properties and characterization of electrically conductive nanocellulose-based composite films. *Fillers and Reinforments for Advanced Nanocomposites.* Woodlands Publishing Series in Composites Science and Engineering. p 3-25.

Manzanares, P (2020). The role of biorefinering research in the development of a modern bioeconomy. *Acta Innov.*, *37*: 47-56.

Milanez, M; Dias, Á; Cristina, K; Carvalho, C De; Jacobus, H; Voorwald, C; Odila, M and Ciof, H (2019). Obtainment and characterization of nanocellulose from an unwoven industrial textile cotton waste: Effect of acid hydrolysis conditions. *Int. J. Biol. Macrom.*, *126*: 496-506.

Mousavi, M, Antxustegi, M M and Labidi, J (2022). Chemosphere nanocellulose-based sensing platforms for heavy metal ions detection : A comprehensive review. *Chemosphere*, *302(January)*: 134823.

Onkarappa, H S; Prakash, G K; Pujar, G H; Rajith Kumar, C R; Radha V and Betageri, V S (2020). Facile synthesis and characterization of nanocellulose from *Zea mays* husk. *Polym. Compos.*, *41(8)*: 3153-3159.

Owi, W T; Ong, H L; Sam, S T; Villagracia, A R; Tsai, C-kuo and Akil, H M (2019). Unveiling the physicochemical properties of natural *Citrus aurantifolia* crosslinked tapioca starch/nanocellulose bionanocomposites. *Ind. Crops Prod.*, *139(October 2018)*: 111548.

Silveira, M H L; Morais, A R C; Da Costa Lopes, A M; Olekszyszen, D N; Bogel-Łukasik, R; Andreaus, J and Pereira Ramos, L (2015). Current pretreatment technologies for the development of cellulosic ethanol and biorefineries. *ChemSusChem*, *8(20)*: 3366-3390.

Trache, D; Tarchoun, A F; Derradji, M, Hamidon, T S; Masruchin, N; Brosse, N and Hussin, M H (2020). Nanocellulose : From fundamentals to advanced applications. *Front. Chem.*, *8*: Article 392.

Velásquez-Cock, J; Gómez H., B E; Posada, P; Serpa G A; Gómez H C; Castro, C; Gañán, P and Zuluaga, R (2018). Poly (vinyl alcohol) as a capping agent in oven dried cellulose nanofibrils. *Carbohydr. Polym.*, *179*: 118-125.

Vivian Abiaziem, C; Bassey Williams, A; Ibijoke Inegbenebor, A; Theresa Onwordi, C; Osereme Ehi-Eromosele, C and Felicia Petrik, L (2019). Preparation and characterisation of cellulose nanocrystal from sugarcane peels by XRD, SEM and CP/MAS 13C NMR. *J. Phys. Conf. Ser.*, *1299(1)*: 012123.

Wu, D; Wei, Z; Zhao, Y; Zhao, X; Mohamed, T A; Zhu, L; Wu, J; Meng, Q; Yao, C and Zhao, R (2019). Improved lignocellulose degradation efficiency based on Fenton pretreatment during rice straw composting. *Bioresour. Technol.*, *294(August)*: 122132.

Wulandari, W T; Rochliadi, A and Arcana, I M (2016). Nanocellulose prepared by acid hydrolysis of isolated cellulose from sugarcane bagasse. *IOP Conference Series: Materials Science and Engineering*, *107*: 012045.

Xiao, J; Li, H; Zhang, H; He, S; Zhang, Q; Liu, K; Jiang, S; Duan, G and Zhang, K (2022). Nanocellulose and its derived composite electrodes toward supercapacitors: Fabrication, properties and challenges. *J. Bioresour. Bioprod.*, *7(4)*: 245-269.

You, A; Chen, W; Voon, H; Sharifah, L and Abd, B (2016). Facile production of nanostructured cellulose from *Elaeis guineensis* empty fruit bunch via one pot oxidative-hydrolysis isolation approach. *Carbohydr. Polym., 157*: 1511-1524.

Zhao, Y; Lei, H; Liu, Y; Ruan, R; Qian, M; Huo, E; Zhang, Q; Huang, Z; Lin, X; Wang, C; Mateo, W and Villota, E M (2020). Microwave-assisted synthesis of bifunctional magnetic solid acid for hydrolyzing cellulose to prepare nanocellulose. *Sci. Total Environ.*, *731*: 138751.

Zhong, C; Zajki-Zechmeister, K and Nidetzky, B. (2021). Reducing end thiol-modified nanocellulose: Bottom-up enzymatic synthesis and use for templated assembly of silver nanoparticles into biocidal composite material. *Carbohydr. Polym.*, *260*: 117772.